Electronic physisorption at plasma walls

Rafael L. Heinisch, Franz X. Bronold, and Holger Fehske

Institut für Physik, Ernst-Moritz-Arndt-Universität Greifswald, D-17489 Greifswald

We model the build-up of the negative surface charge at a plasma wall as an electronic physisorption process. Quite often the wall is supposed to be a perfect absorber for ions and electrons. To improve this ad hoc assumption, we calculate for electrons the sticking coefficient and desorption time for phonon-mediated physisorption, as it is appropriate for dielectric surfaces. We present results for the initial stages of the charging process, where the wall carries no charges yet, and for a charged wall. For the case of an uncharged wall we find $s_e \ll 1$ and $\tau_e \approx 10^{-4} s$, while for a charged wall we obtain $\tau_e \approx 0$ and $s_e \approx 0.1$. Thus in both cases we observe a significant correction to a perfect absorber.

1. Motivation

Plasma walls collect electrons more efficiently than ions and thereby acquire a negative surface charge leading to the creation of a plasma sheath in front of the wall. Moreover, the negative surface charge also represents a reservoir for secondary electron emission or surface supported electron-ion recombination. In view of the importance of surface charges, for instance, in dusty plasmas [1] or solid-state based microdischarges [2], a microscopic understanding of the processes leading to a negative surface charge is a necessary prerequisite for a complete kinetic modelling of a bounded plasma.

Despite the importance of the negative surface charge, there is, as of now, only a loose understanding of its build-up. A common assumption [3] is that all incident electrons and ions are adsorbed at the wall where they recombine instantly. The wall potential is the potential which balances electron and ion flux from the plasma.

Based on the idea of a two-dimensional surface plasma [4, 5], we suggest to consider the build-up of a negative surface charge as an electronic physisoprtion process at the surface. In this model the ion and electron surface densities satisfy coupled rate equations,

$$\frac{\mathrm{d}}{\mathrm{d}t} n_{e,i} = s_{e,i} j_{e,i} - \frac{1}{\tau_{e,i}} n_{e,i} - \alpha_{RW} n_i n_e \ , \qquad (1)$$

where $s_{e,i}$ and $\tau_{e,i}$ are the sticking coefficient and the desorption time for electrons and ions, respectively, and α_{RW} is the recombination constant.

Assuming a collisionless planar sheath, the two equations (1) reduce in equilibrium to

$$s_e j_e^{\mathrm{th}} = s_i j_i^B + \frac{n_e}{\tau_e} - \frac{n_i}{\tau_i} \ , \qquad (2)$$

where j_e^{th} is the thermal electron flux and j_i^B is the mono-energetic ion flux from the plasma.

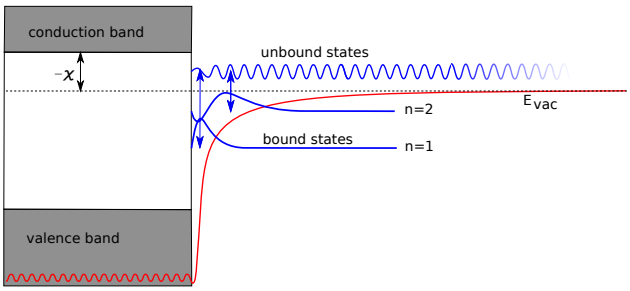

Fig. 1: Sketch of the potential (red) and electronic states (blue) at an uncharged dielectric surface.

We believe microscopic processes at the wall to be most relevant for the calculation of s_e and τ_e since electrons can more easily explore the potential close to the surface or even penetrate the surface.

In view of the importance of dielectric walls for dielectric barrier discharges (MgO, SiO_2 or Al_2O_3) or dusty plasmas (graphite or melamine-formaldehyde) we have studied sticking and desorption of an electron on a dielectric surface. In the following, we will consider electronic physisorption at uncharged and charged plasma walls.

2. Uncharged wall

In the beginning of the charging process, there are no electrons residing on the wall yet. In this case, the polarisation-induced electron-surface interaction yields the image potential,

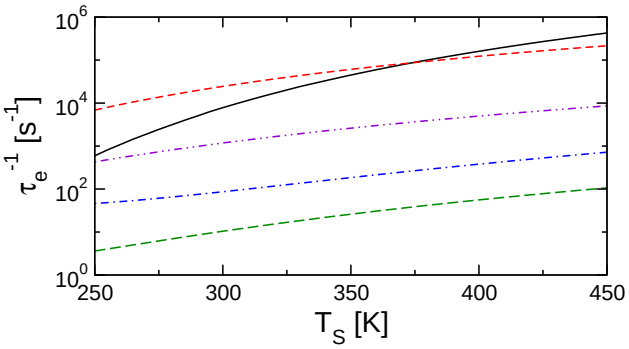

Fig. 2: Inverse desorption time τ_e^{-1} as a function of the surface temperature T_S for graphite, MgO, Al_2O_3, CaO, and SiO_2 (legend see figure 3).

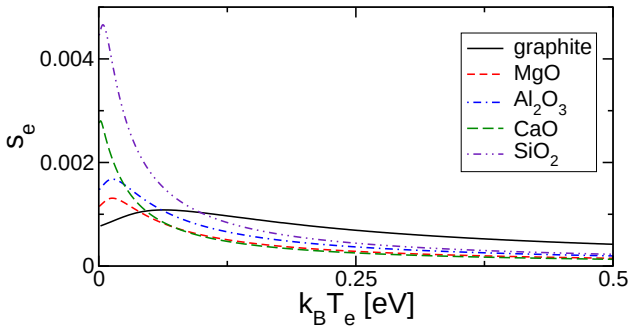

Fig. 3: Prompt energy-averaged sticking coefficient for graphite, MgO, Al_2O_3, CaO, and SiO_2 as a function of the mean energy of the electron at $T_S = 300K$.

$V(z) = -(\epsilon-1)e^2/4(\epsilon+1)z$, which gives rise to a Rydberg series of bound image states. If the conduction band minimum is above the vacuum level, that is, for negative electron affinity χ, as it is the case for the alkaline earth oxides, the image states are the lowest unoccupied states allowing for the temporary trapping of electrons.

Transitions among bound surface states and bound and continuum states are due to a dynamic perturbation of the surface potential triggered by an acoustic phonon leading to an oscillation of the image plane. Figure 1 illustrates the electronic states and transitions at the surface.

The starting point for the calculation of the sticking coefficient and the desorption time is a quantum kinetic rate equation for the occupancy of the image states [6]. The time dependence of the bound state occupancy is given by

$$\begin{aligned}\frac{\mathrm{d}}{\mathrm{d}t}n_n(t) &= \sum_{n'}\left[W_{nn'}n_{n'}(t) - W_{n'n}n_n(t)\right] \\ &\quad - \sum_k W_{kn}n_n(t) + \sum_k \tau_t W_{nk} j_k(t) \\ &= \sum_{n'} R_{nn'}n_{n'}(t) + \sum_k \tau_t W_{nk} j_k(t)\ , \quad (3)\end{aligned}$$

where $W_{nn'}$ is the transition probability from one bound state n' to another bound state n, W_{kn} and W_{nk} are the transition probabilities from the bound state n to the continuum state k and vice versa and τ_t is the transit time through the surface potential. The occupancy of the bound states evolves according to the eigenvalues λ_κ of the matrix $R_{nn'}$ which is defined implicitly by the above equation. It turns out that $n_n(t)$ contains a quickly and a slowly varying part. On the slow time scale the total bound state occupancy is given by

$$\frac{\mathrm{d}}{\mathrm{d}t}n^s(t) = \sum_k s_{e,k}^{\mathrm{kinetic}} j_k(t) - \frac{1}{\tau_e}n^s(t) \qquad (4)$$

with $\tau_e = \lambda_0^{-1}$ the desorption time and $s_{e,k}^{\mathrm{kinetic}} = \tau_t \sum_{n,l} e_n^{(0)} \tilde{e}_l^{(0)} W_{lk}$ the kinetic sticking coefficient; $e_n^{(0)}$ and $\tilde{e}_n^{(0)}$ are the right and left eigenvectors to the smallest eigenvalue λ_0 of $R_{nn'}$. The kinetic sticking coefficient gives the probability for an electron to be trapped and to relax in the image states. The probability only for trapping is given by the prompt sticking coefficient, $s_{e,k}^{\mathrm{prompt}} = \tau_t \sum_n W_{nk}$.

To obtain the sticking coefficient and the desorption time from the above formalism, the remaining task is to calculate the transition probabilities $W_{nn'}$. Due to the large potential depth with respect to the maximum phonon energy for the materials we consider, we need to calculate transition probabilities for multi-phonon processes. To this end, we have used an expansion of the T matrix which is feasible for two-phonon processes [7] and a nonperturbative approximation based on the nonlinear electron-phonon interaction for higher order processes [8].

In Figs. 2 and 3 we give an overview of our results for graphite, MgO, Al_2O_3, CaO and SiO_2. Figure 2 shows the inverse desorption time as a function of the surface temperature. For all materials, desorption benefits from a higher surface temperature. Desorption tends to be faster if two-phonon processes link the lowest two bound states (graphite and magnesium oxide) instead of three-phonon processes (aluminum oxide, calcium oxide and silicon oxide). Figure 3 shows the prompt energy-averaged sticking coefficient as a function of the energy of a Boltzmann distributed electron.

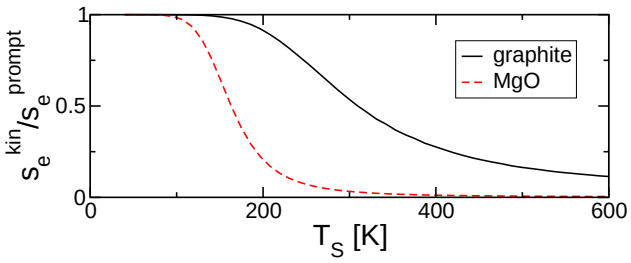

Fig. 4: Ratio of the kinetic to the prompt energy averaged sticking coefficient as a function of the surface temperature for $k_B T_e$=0.1 eV showing a relaxation bottleneck for high surface temperatures.

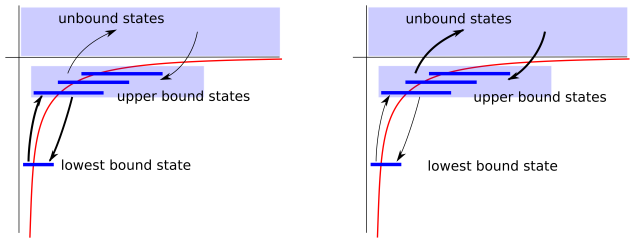

Fig. 5: Sketch of the electron kinetics at the uncharged wall for low temperature (left) and high temperature (right). Bold arrows show the dominant transitions.

Our results show, that in the in very beginning of charge collection, the wall is not a perfect absorber and the desorption time and the sticking coefficient differ significantly from their perfect absorber values, that are $s_e = 1$ and $\tau_e^{-1} = 0$.

Focussing on the effect of the potential depth and the surface temperature, we have studied the electron kinetics in the image states in detail [7, 8]. The initial trapping of electrons, characterised by the prompt sticking coefficient, occurs via one-phonon processes in the upper bound states. Multi-phonon processes contribute very little to the sticking coefficient. Initial trapping is relatively insensitive to the potential depth and the surface temperature, contrary to desorption and relaxation of a trapped electron in the bound states. Varying the potential depth we can identify the dominant desorption channel: The direct transition from the lowest bound state to the continuum dominates only if it is enabled by a one-phonon transition. As soon as there is no direct one-phonon link to the continuum, as it is the case for almost all dielectrics of practical interest, desorption proceeds via cascades over the upper bound states.

Relaxation after trapping but before desorption depends on the strength of the transitions from the upper bound states to the lowest bound state versus the strength of the transitions to the continuum. If the lowest two bound states are linked by a one-phonon process the electron relaxes for all temperatures. If a multi-phonon process is required, as it is the case for all the materials we consider, a relaxation bottleneck can occur. Figure 4 shows the ratio $s_e^{\mathrm{kin}}/s_e^{\mathrm{prompt}}$, which gives the probability of relaxation before desorption, indicating inhibited relaxation for high temperatures.

Figure 5 summarises the electron kinetics at uncharged walls. For low temperatures a trapped electron relaxes to the bottom and desorbs in cascades, for high temperatures relaxation is inhibited and the trapped electron has only a small chance to fall to the lowest bound state. Instead, it desorbs from the upper bound states.

3. Charged wall

The physisorption scenario we have considered so far applies to an uncharged wall. Over the course of the charging process a plasma wall acquires a wall potential of typically a few electron volts. The surface potential now consists of the image potential and a Coulomb barrier due to the electrons already residing on the wall. Due to the wall potential the energy of the image states is raised and they overlap with empty states in the conduction band. The lowest unoccupied electronic states are now inside the conduction band. Electron trapping can still be considered as a physisorption process. However, trapping takes place no longer in surface but in bulk states and instead of surface vibrations electron energy relaxation is now enabled by bulk phonon modes.

In order for an electron to reach the surface, its energy has to exceed the wall potential ϕ_w. When it reaches the surface it penetrates the surface up to a depth L_e before it is either reflected or trapped. Assuming optical phonons to be the dominant scattering mechanism in the wall and neglecting multi-phonon transitions, electrons with energy in the interval $[\phi_w, \phi_w + \omega_{ph}]$, with ω_{ph} the phonon frequency, can get trapped by phonon emission. Once below ϕ_w the electron will quickly trickle down to the conduction band minimum. Transitions from the conduction band to the continuum are only possible for electrons with energy in the interval $[\phi_w - \omega_{ph}, \phi_w]$. As these high lying states are only very sparsely

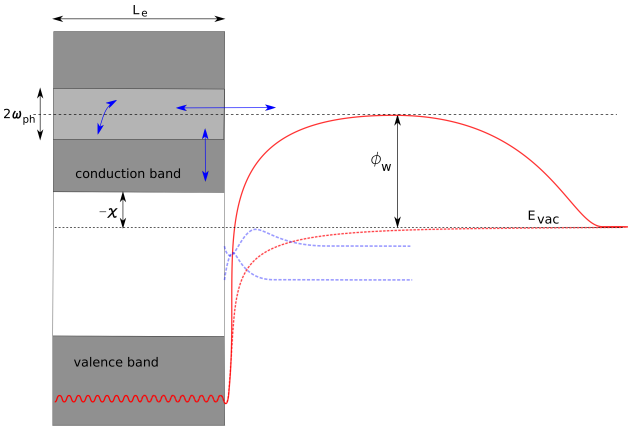

Fig. 6: Sketch of the physisorption process at a charged wall. The dotted lines correspond to the uncharged wall.

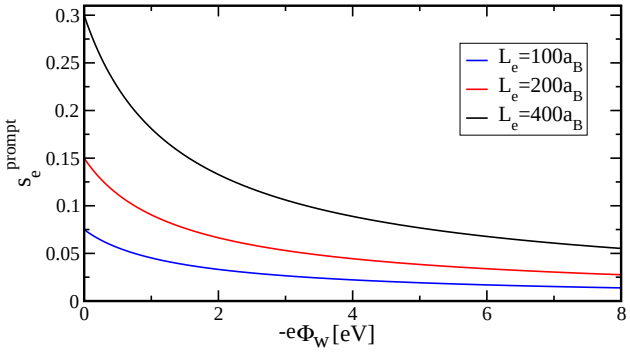

Fig. 7: Prompt electron sticking coefficient for Al_2O_3 at room temperature as a function of the wall potential ϕ_w and the electron penetration length L_e [9].

populated, the desorption time will be very long approaching $\tau_e^{-1} = 0$, in agreement with the perfect absorber model (see below however). Figure 6 gives a sketch of physisorption at a charged wall.

A first estimate for the desorption time and the sticking coefficient can be obtained from the bulk electron-phonon coupling [9]. They are given by

$$s_e = \frac{\sum_{\vec{K}k\vec{Q}q} \frac{2L_e m^*}{\hbar k} W^+(\vec{Q}q, \vec{K}k) \exp\left[-\beta_e E_{\vec{K}k}\right] k}{\sum_{\vec{K}'k'} \exp\left[-\beta_e E_{\vec{K}'k'}\right] k'}$$

$$\frac{1}{\tau_e} = \frac{\sum_{\vec{Q}q\vec{K}k} W^-(\vec{K}k, \vec{Q}q) e^{\left[-\beta_{\rm eff}(\tau_e^{\rm th}) E_{\vec{Q}q}\right]}}{\sum_{\vec{Q}'q'} e^{\left[-\beta_{\rm eff} E_{\vec{Q}'q'}\right]}} \qquad (5)$$

where $\vec{Q}q$ labels bound and $\vec{K}k$ unbound states and $W^{\pm}(\vec{k}, \vec{k}')$ are the transition probabilities explicitly given in [9].

Figure 7 shows the sticking coefficient for Al_2O_3 as a function of the wall potential. As the penetration depth L_e enters our estimate as a parameter we plot s_e for typical values of L_e measured in tunnelling diode experiments. Compared to the uncharged wall the sticking coefficient is now on the order of 10^{-1} instead of 10^{-4}. Nevertheless the wall is still not a perfect absorber. Using the balance equation (2) we find that the wall potential amounts to about one third of the surface potential for a perfect absorber [9].

4. Conclusions

We have considered the build-up of a negative surface charge as an electronic physisorption process. Initially the wall is essentially uncharged. In this case, external surface states - image states - can trap electrons. Transitions involving the image states are triggered by surface vibrations. We find $s_e \approx 10^{-4}$ and $\tau_e \approx 10^{-4} s$ showing a significant deviation from the perfect absorber model. At a later stage of the charging-up when the wall is already charged, internal states are available for trapping and energy relaxation is enabled by bulk phonons. In this case $\tau_e^{-1} \approx 0$ and $s_e \approx 10^{-1}$. The charging process begins with electron trapping in the image states and the surface charge is located in front of the surface. With increasing wall potential internal states contribute to trapping. The surface charge is now located in a layer beneath the surface and the desorption time and sticking coefficient are much closer to the perfect absorber values.

This work was supported by the Deutsche Forschungsgemeinschaft through SFB/TRR 24.

References

[1] V. E. Fortov *et al.*, Phys. Rep. **421** (2005) 1.
[2] M. J. Kushner, J. Phys. D. **38** (2005) 1633.
[3] R. N. Franklin, Plasma phenomena in gas discharges (Clarendon, Oxford) (1976).
[4] K. G. Emeleus, J. R. M. Coulter, Int. J. Electronics **62** (1987) 225.
[5] J. F. Behnke *et al.*, Contrib. Plasma Phys. **37** (1997) 345.
[6] Z. W. Gortel *et al.* , Phys. Rev. B. **22** (1980) 5655.
[7] R. L. Heinisch *et al.*, Phys. Rev. B **81** (2010) 155420, Phys. Rev. B **82** (2010) 125408.
[8] R. L. Heinisch *et al.*, to be published.
[9] F. X. Bronold *et al.*, IEEE Trans. Plasma Science **39** (2011) 644.